13

A High Frequency AC-AC Converter for Inductive Power Transfer (IPT) Applications

Hao Leo Li, Patrick Aiguo Hu and Grant Covic
The University of Auckland, New Zealand

1. Introduction

A contactless power transfer system has many advantages over conventional power transmission due to the elimination of direct electrical contacts. With the development of modern technologies, IPT (Inductive Power Transfer) has become a very attractive technology for achieving wireless/contactless power transfer over the past decade and has been successfully employed in many applications, such as materials handling, lighting, transportation, bio-medical implants, etc. (Kissin et al. 2009; Li et al. 2009).
A typical configuration of an IPT system is shown in Fig.1. The system comprises two electrically isolated sections: a stationary primary side, and a movable secondary side.

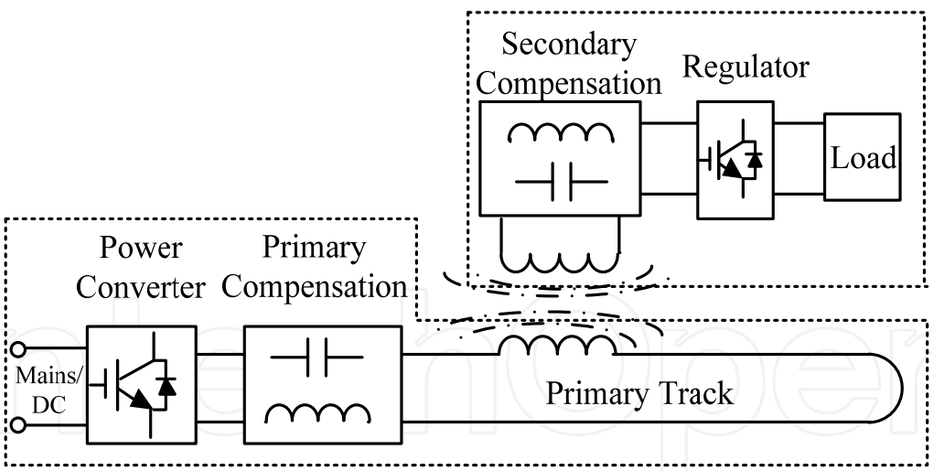

Fig. 1. Typical configuration of a contactless power transfer system.

The stationary primary side is connected to a front-end low frequency power source, which is usually the electric utility at 50Hz or 60Hz, single-phase or three-phase. For some special applications, the power source can be a DC source or a battery. The primary side consists of a high frequency power converter which generates and maintains a constant high frequency AC current in a compensated conductive track loop/coil normally within the range from 10 kHz-1MHz (Dawson et al. 1998; Dissanayake et al. 2008). The pickup coil of the secondary side is magnetically coupled to the primary track to collect energy. The reactance of the secondary side increases proportionally with an increase in operating frequency, and as

such is normally compensated by other capacitors or inductors. In order to have a controlled output for different loads, usually a switch mode regulator is used on the secondary side to control the power flow and maintain the output voltage to be constant.

At present, a DC-AC inverter is a common solution to generate a high frequency track current for an IPT system. Often a front-end low frequency mains power source is rectified into a DC power source, and then inverted to the required high frequency AC track current. Energy storage elements, such as DC capacitors, are used to link the rectifier and the inverter. These energy storage elements cause the AC-DC-AC converters to have some obvious drawbacks such as large size, increased system costs, and more complicated dynamic control requirements in practical applications. In addition, those extra components and circuitry reduce the overall efficiency of the primary converter. Having an IPT power supply without energy storage is an intrinsically safe approach for applications and desirable.

Ideally an direct AC-AC converter would be a good alternative to obtain this high frequency power directly from the mains (Kaiming & Lei 2009). A matrix structure eliminates the need for the DC link, but the synchronization between the instantaneous input and output becomes very difficult, and the quality of the output waveform is usually poor due to complicated switching combinations involved (Hisayuki et al. 2005). Furthermore, the circuit transient process involved in the traditional forced switched matrix converters is normally complex and difficult to analyse. The control complications and synchronization limitations make traditional matrix converters unsuitable for IPT systems.

This chapter presents a direct AC-AC converter based on free circuit oscillation and energy injection control for IPT applications. A simple but unique AC-AC topology is developed without a DC link. A variable frequency control and commutation technique is developed and discussed. The detailed circuit model and the converter performance are analysed.

2. Fundamentals of circuit oscillation and energy injection control

Most of the existing converters for IPT applications are resonant converters, where the track is tuned with one or more reactive components in series, parallel or hybrid connection. Regardless of the tuning method, if a resonant tank is oscillatory, even without excitation, a resonant current will oscillate freely provided some energy is stored initially in the resonant tank. A simple free oscillation path can be naturally formed by connecting a capacitor or a tack inductor. This can be achieved in many ways using a switching network.

Fig.2 shows a basic configuration of a voltage sourced energy injection and free oscillation inverter. It comprises a power supply, a switching network and a resonant tank consisting of a track inductor L, a capacitor C and a resistor R.

The inverter has two operating modes: energy injection and free oscillation. When terminals a and b are connected to the power source by the switching network during a suitable period, energy can be injected into the resonant tank. However, when the terminals a and b are shorted by the switching network, the track inductor L, its tuning capacitor C and the resistor R form a free oscillation network, which is decoupled from the power supply. The stored energy in the closed path of a resonant tank will oscillate in the form of an electric field in the capacitor and magnetic field in the inductor, and finally will be consumed by the equivalent resistance which represents the load and the ESR. To maintain the required energy level in the resonant tank for sustained oscillation and energy transfer to any attached loads, more energy is required to go into the tank by reconfiguring the switch

network to connect to the power source. From an energy balance point of view, such an operation based on discrete energy injection and free oscillation control is very different from normal voltage or current fed inverters. Therefore, the controller design and performance of the inverters based on this approach are very different from other traditional controllers as well.

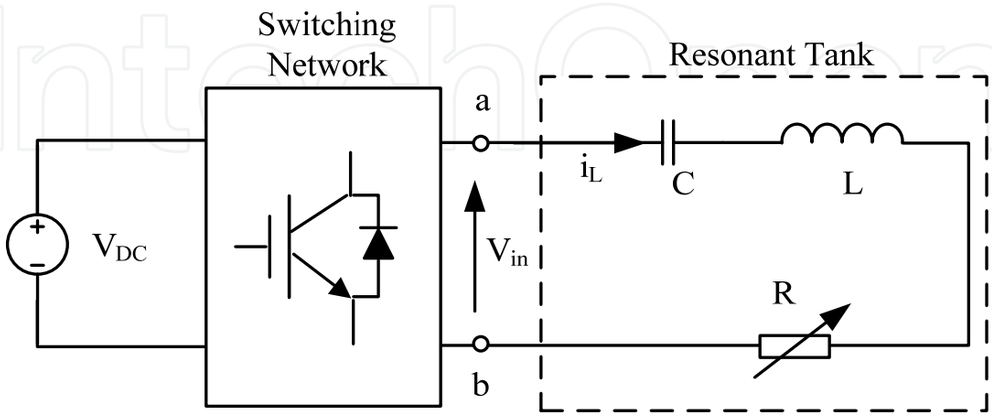

Fig. 2. Principle diagram of injection method of voltage source.

The inverter has two operating modes: energy injection and free oscillation. When terminals a and b are connected to the power source by the switching network during a suitable period, energy can be injected into the resonant tank. However, when the terminals a and b are shorted by the switching network, the track inductor L, its tuning capacitor C and the resistor R form a free oscillation network, which is decoupled from the power supply. The stored energy in the closed path of a resonant tank will oscillate in the form of an electric field in the capacitor and magnetic field in the inductor, and finally will be consumed by the equivalent resistance which represents the load and the ESR. To maintain the required energy level in the resonant tank for sustained oscillation and energy transfer to any attached loads, more energy is required to go into the tank by reconfiguring the switch network to connect to the power source. From an energy balance point of view, such an operation based on discrete energy injection and free oscillation control is very different from normal voltage or current fed inverters. Therefore, the controller design and performance of the inverters based on this approach are very different from other traditional controllers as well.

In principle, any power source may be used to generate high frequency currents apart from a DC source using free oscillation and energy injection control providing the converter topologies are properly designed. For such a reason, if the energy injection control and free oscillation is well coordinated, the energy storage components of an AC-DC-AC converter can be fully eliminated. Therefore, an AC power source can be directly used to generate a high frequency AC current for an IPT system. As a result, the cost, size and efficiency of a primary IPT converter can be significantly improved.

Eliminating the front-end AC-DC rectification and DC storage capacitors, a conceptual AC converter based on energy injection control can be created as shown in Fig. 3.

It can be seen from Fig.3 that an AC source is directly connected to a resonant network by switches. The design of the switching topology could be very critical here to ensure the

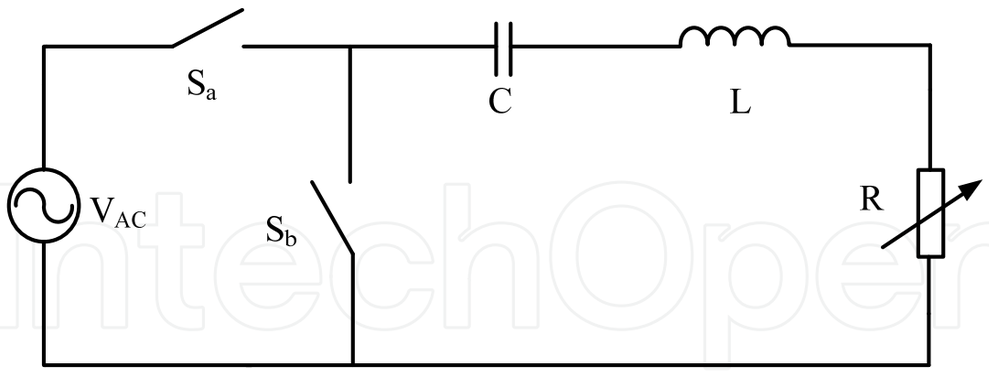

Fig. 3. A conceptual direct AC-AC converter with energy injection control.

energy can be injected according to the load requirements, and to ensure that energy flowing back to the power source is prevented during circuit oscillation.

In practice, most semiconductor switches such as IGBTs and MOSFETs have anti-parallel body diodes. Such a structure ensures the switches can operate bi-directionally but with only one controllable direction. With a combination of the IGBTs or MOSFETs, an AC switch can be constructed to achieve bidirectional controllability (Sugimura et al. 2008). There are many combinations of an AC switches can be used to replace the ideal switches in Fig. 3. After taking the practical consideration of implementation such as control simplicity, cost and efficiency into consideration, the proposed converter topology is developed as shown in Fig. 4, which consists of minimum count of four semiconductors.

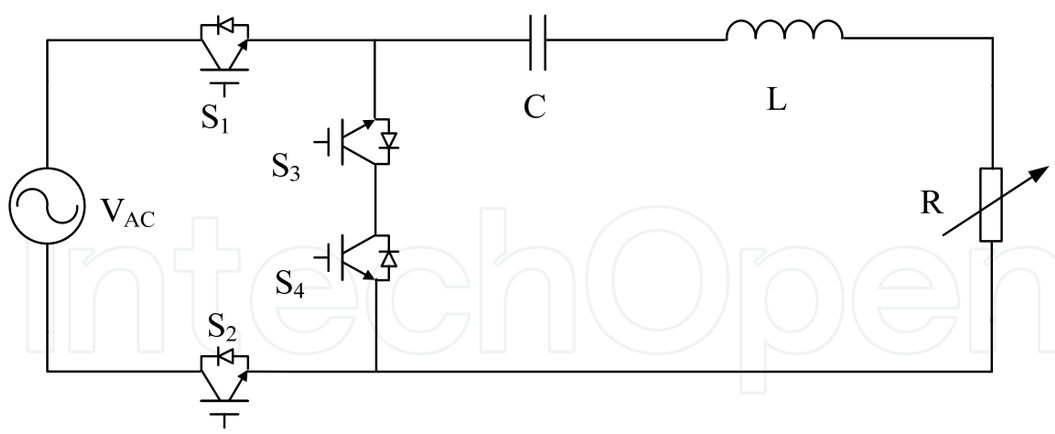

Fig. 4. A typical configuration of a direct AC-AC converter.

The ideal switch Sa in Fig. 3 is presented by an AC switch S1 and S2 as shown in Fig. 4. The ideal switch Sb is replaced by S3 and S4 to construct a free oscillation path for the current. By turning on/off the switches through a properly designed conduction combination, the energy injection and free oscillation can be maintained while the undesired energy circulation to the source can be prevented. The detailed control scheme for all those switches is discussed in the following section.

3. Operation principles

3.1 Normal switching operation

The proposed AC-AC converter is based on a direct conversion topology without a middle DC link. Therefore, the commutation and synchronization of the source voltage and resonant loop branches needs to be considered. To determine the switch operation, it is necessary to identify the polarity of the input voltage and the resonant current. According to the polarity of the low frequency input voltage and the resonant track current, the converter operation can be divided into four different modes as shown in Fig.5.

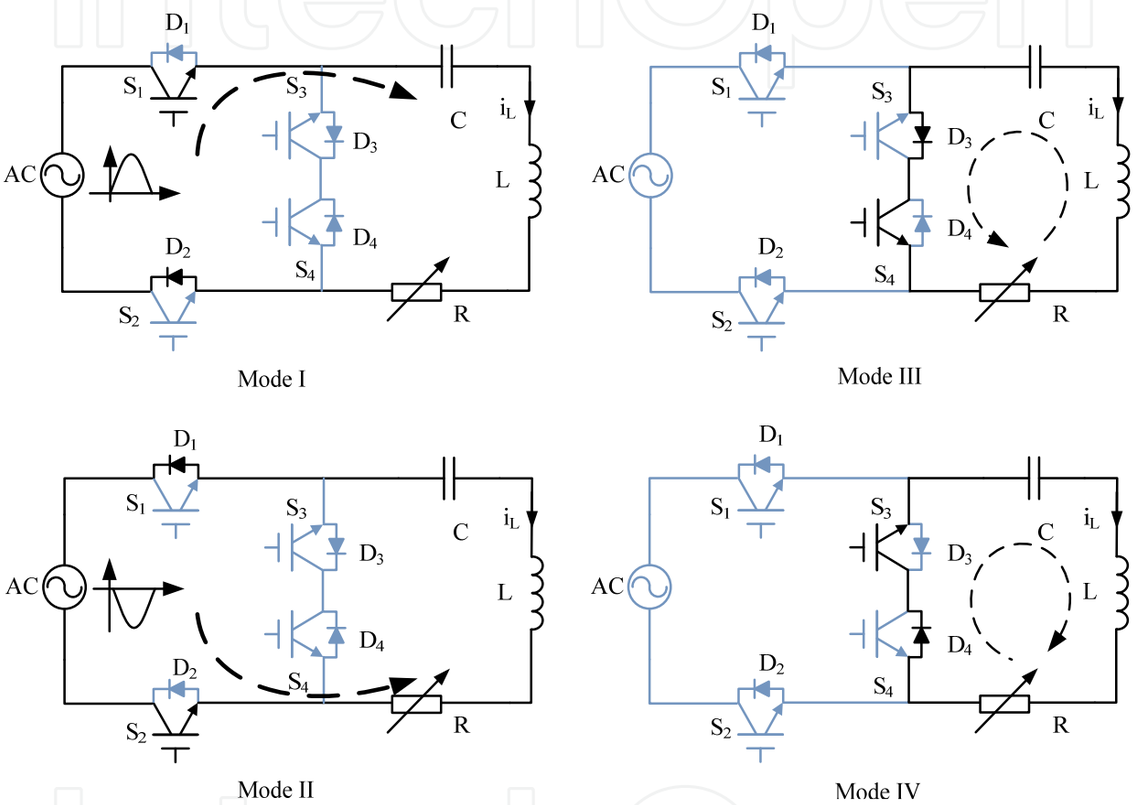

Fig. 5. Switch operation of AC-AC converter.

In Fig.5, Mode III and Mode IV present the current free oscillation in different directions. Mode I and Mode II are the states to control the energy injection based on the different polarities of the input voltage, which is also determined by the directions of the resonant current.

A typical current waveform of the converter and the associated switching signals when the input voltage is in the positive polarity are shown in Fig. 6.

In Fig. 6, if the negative peak value of the resonant current is smaller than the designed reference value -Iref in t1, switch S1 is turned on in the following positive cycle when $V_{AC}>0$, while S2, S3 and S4 remain off. As such, the instantaneous source voltage V_{AC} is added to the resonant tank. This operation results in a boost in the resonant current during t2. Regardless of whether the peak current is smaller or greater than the reference value -Iref, the operation of the converter in the next half cycle of t3 would automatically be switched to Mode III, where switch S3, S4 are on and S1, S2 are turned off, such that the L-C-R forms a

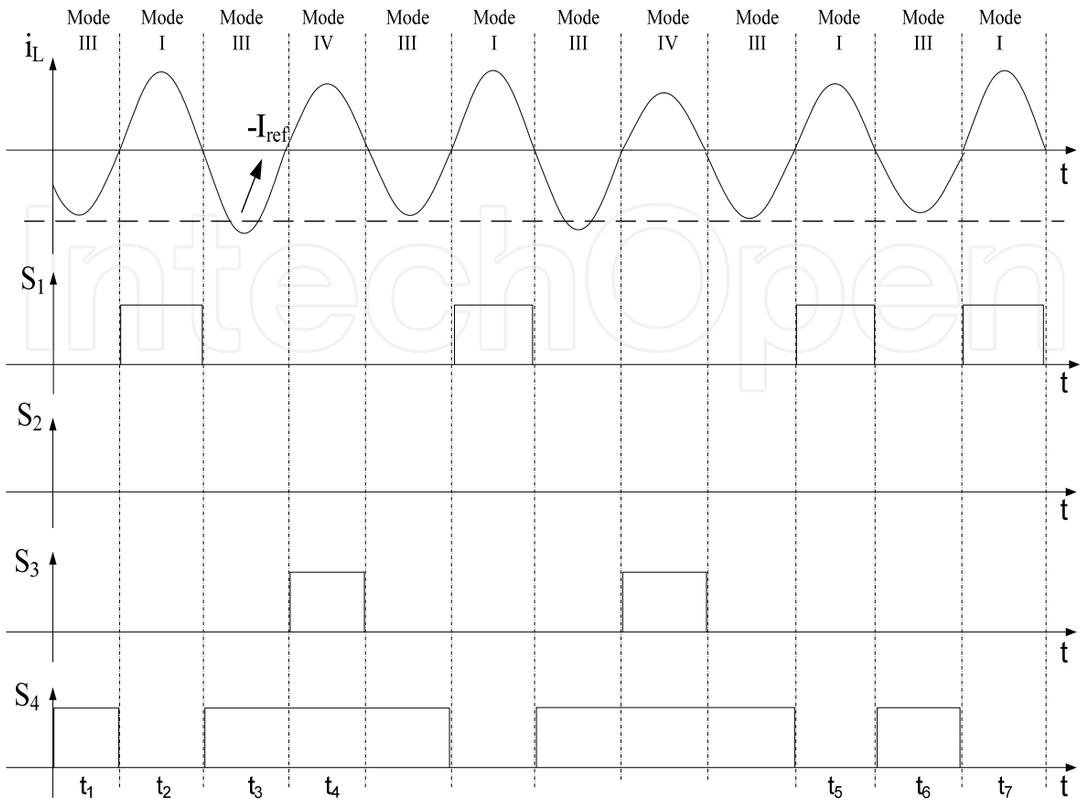

Fig. 6. Converter operation when input voltage V_{AC}>0.

free oscillation circuit enabling the energy to circulate between the capacitor C and inductor L. However, if the peak current is larger than the reference -Iref at t3, the converter operates in Mode IV at the next half cycle of t4. If the negative peak current is still smaller than the reference -Iref after a positive energy injection (for example, peak current is still very small at t6 even after the injection at t5, and more energy is still needed in the next positive half cycles of t7.), then, the converter will operate at Mode I at t7, and continue to repeat the operation between Mode I and Mode III in the following half cycles until its peak magnitude larger than the predefined reference value.

The operation of the converter is similar to the situation when the input voltage V_{AC}<0. The only difference is that S2 is used to control the negative input voltage which is applied to the resonant tank when the resonant current is negative. Additionally, the peak current would be compared to $+I_{ref}$ to determine if the converter is operated between Mode II/Mode IV, or Mode IV and Mode III. The selection of the mode during normal operation for both positive and negative input is summarized and shown in Fig.7.

3.2 Switching commutation

The proposed converter inherits the simple matrix structure with less switching components and without commutation capacitors. By utilizing the body diodes of each switch, the circuit resonant current can be naturally maintained, even the switches operate at non ZCS condition. Like a DC-AC inverter, variable frequency control can also be employed in the AC-AC converter. Switches being operated under such a condition are switched at the zero

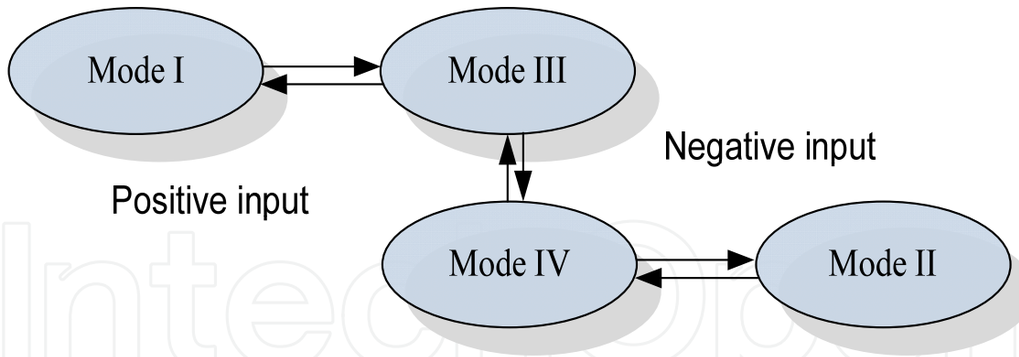

Fig. 7. Mode selection diagram during normal operation.

crossing points to follow the resonance of the current so as to keep the magnitude of the current constant. Nevertheless, the variable frequency switching control also faces problems as a result of the frequency shift (Hu et al. 2000), which cause uncertainty in the direction of the resonant current when the input voltage is at its zero crossing points. This implies that the current completes an entire half cycle over the zero crossing point of input. The polarity change of the input voltage will make the modes of converter operation vary between energy injection states and free oscillation states. Therefore, it is necessary to consider the best switching commutation technique when a variable frequency control strategy is developed for the proposed AC-AC converter.

Theoretically, the track current may have four possible operating conditions around the zero crossing points of the source voltage according to the current directions and the variation tendency of the input voltage, as follows:

Condition A: The input voltage changes from positive to negative. The current stays positive over the zero crossing point as shown in Fig.8.

Here S1 is on to maintain the current while S3 is to be turned on to continue the current.

Condition B: The input voltage changes from positive to negative. The current stays negative over the zero crossing point as shown in Fig.8.

Here S4 is on to maintain the current while S2 is to be turned on to continue the current.

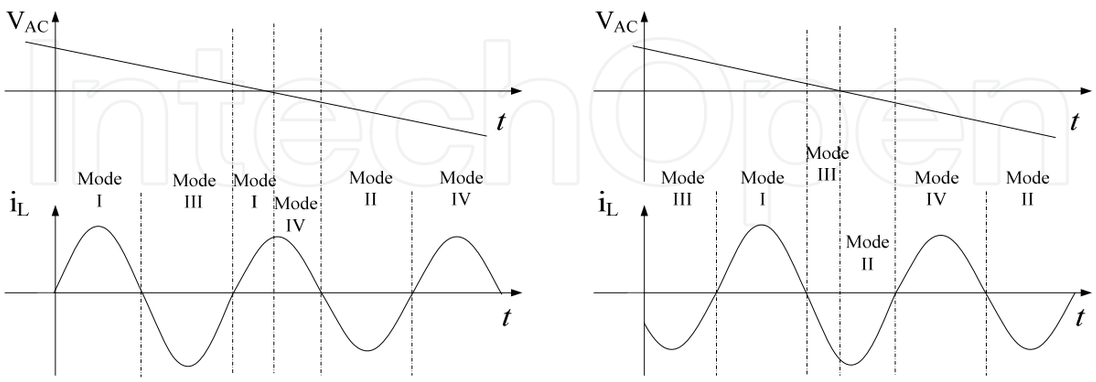

Condition A Condition B

Fig. 8. Operation transient when the input voltage from positive to negative.

Condition C: The input voltage changes from negative to positive. The current stays positive over the zero crossing point as shown in Fig.9.

Here S3 is on to maintain the current while S1 is to be turned on to continue the current.
Condition D: The input voltage changes from negative to positive. The current stays negative over the zero crossing point as shown in Fig.9
Here S2 is on to maintain the current while S4 is to be turned on to continue the current.

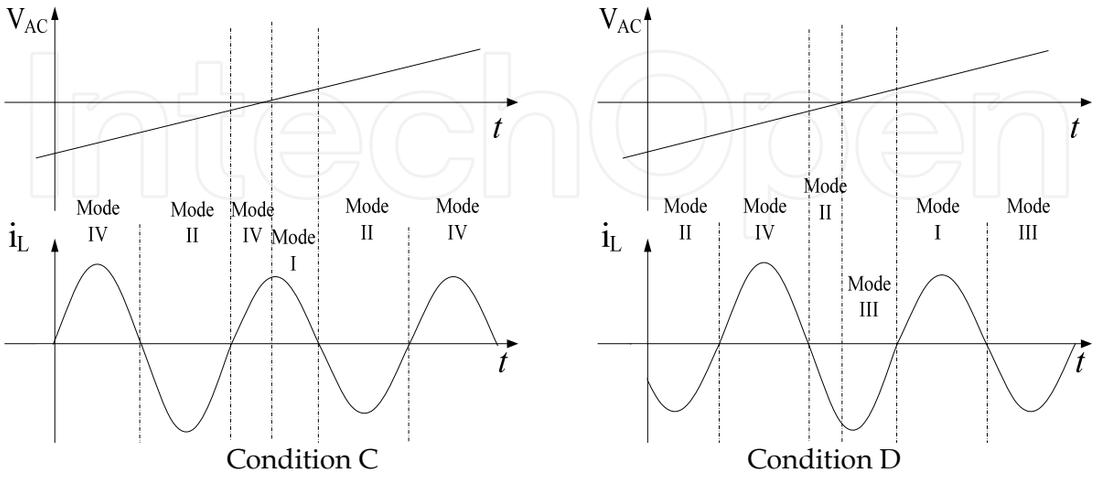

Fig. 9. Operation transient when the input voltage from negative to positive.

It can be seen that there are two additional conditions apart from the normal operation conditions. The operation mode around the zero crossing periods of the input voltage must change between Mode I and Mode IV, or Mode II and Mode III. In fact, the switching commutation between Mode I and Mode IV can be achieved if S3 is always on when the input voltage is in the positive polarities. Similarly, the switching commutation between Mode II and Mode III also can be achieved by keeping S4 on if the input voltage is negative. Such switch operations can maintain the oscillation without affecting normal operation.
From the above discussion, the detailed operation of the AC-AC converter for all conditions is listed in Table 1, according to the input voltage, the resonant current and the predefined current reference. Typical waveforms of the converter with a smooth commutation using this variable frequency control strategy are illustrated in Fig. 10.
The detailed shifting relationship between the operation modes during operation can be summarized in Table 1.

Resonant Current	Input Voltage	Switches/Diodes status	Mode
i_L>0, and previous $\hat{i}_L > -I_{ref}$	V_{AC} >0	S1/D2on S2/S3/S4/D1/D3/D4off	Mode I
i_L<0, and previous $\hat{i}_L < +I_{ref}$	V_{AC} <0	S2/D1 on S1/S3/S4/D1/D3/D4off	Mode II
i_L <0	V_{AC} >0	S4/D3on S1/S2/S3/D1/D2/D4off	Mode III
Previous $\hat{i}_L > +I_{ref}$	V_{AC} <0		
i_L <0	V_{AC} <0	S3/D4on S1/S2/S3/D1/D2/D3off	Mode IV
Previous $\hat{i}_L < -I_{ref}$	V_{AC} <0		

Table 1. Switching states of operation modes.

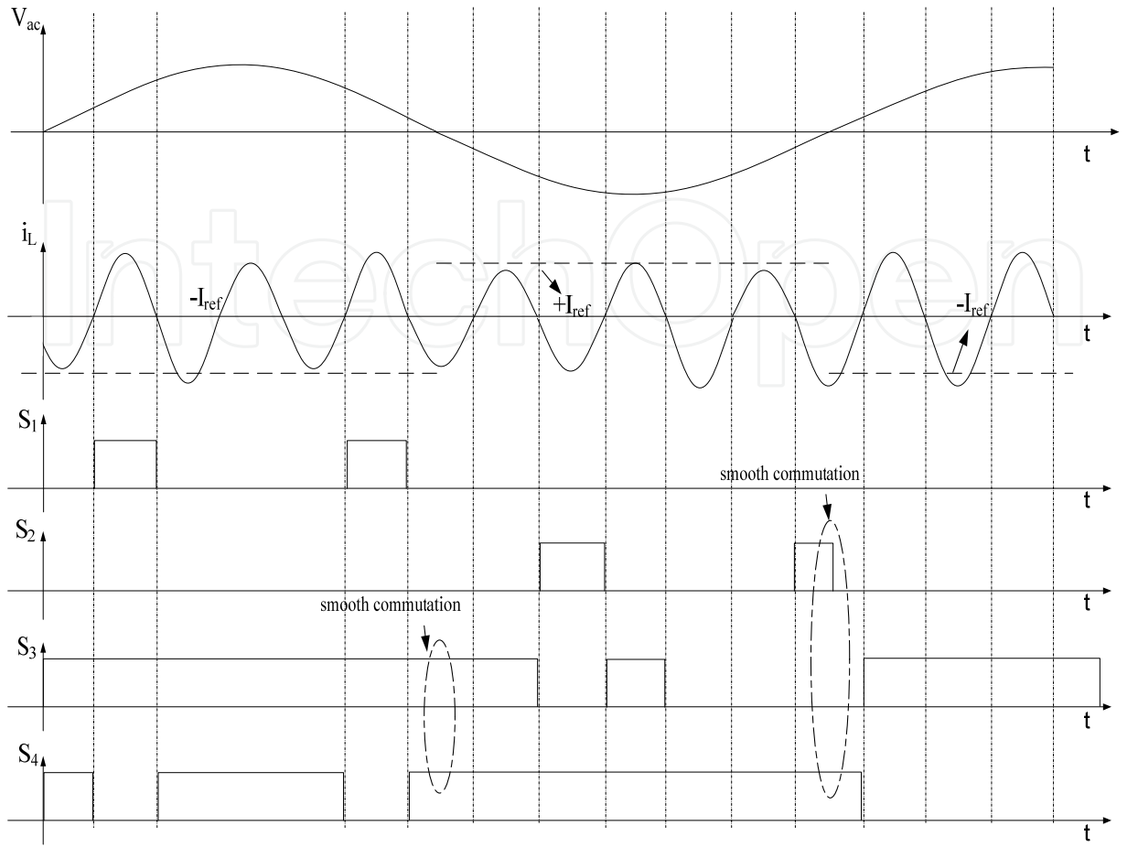

Fig. 10. Waveforms of the converter with smooth commutation.

4. Modeling and analysis

The control strategy of the proposed converter is discrete energy injection control based on the polarity of the input voltage and the resonant current. Since the energy injection occurs discretely, the input phase angle is different for each injection period. During the energy injection period while $V_{AC}>0$, the input voltage is in the same direction as the track current in its positive direction. However, the value of input voltage during each injection varies according to the time instant of the injection. The situation is similar when $V_{AC}<0$; but the track current would be in the negative direction for energy injection. At each injection instant the input voltage over the track can be expressed by the instantaneous value of the AC source as:

$$v_{in}(t) = \hat{V}_{AC} \sin \beta \tag{1}$$

where $\hat{V}_{AC}$ is the peak value of the mains voltage, β=sin(ωt) is the phase angle of the input AC voltage when energy injection occurs. Theoretically, the instantaneous input voltage during each injection period varies between the beginning and the end of the period. This variation in the input is very small if the resonant frequency is much higher than the mains frequency, as is normally the case for IPT systems. For such a reason, the input voltage

applied in each half injection period can be assumed to be constant. The input voltage Vin can therefore be defined as:

$$V_{in} = \begin{cases} \hat{V}_{AC} \sin \beta \\ 0 \end{cases} \tag{2}$$

According to the control strategy of the converter, the differential equations of the equivalent circuit according to the Kirchhoff's voltage law of the circuit can be expressed as:

$$\begin{cases} \dfrac{di_L}{dt} = \dfrac{V_{in}}{L} - \dfrac{Ri_L}{L} - \dfrac{v_C}{L} \\ \dfrac{dv_C}{dt} = \dfrac{i_L}{C} \end{cases} \tag{3}$$

By solving these equations, the instantaneous value of the current during the energy injection and free oscillation periods can be expressed respectively as:

$$i_L = \frac{\hat{V}_{AC} \sin \beta + v_C(0)}{\omega L} e^{-\frac{t}{\tau}} \sin \omega t \tag{4}$$

$$i_L = \frac{v_C(0)}{\omega L} e^{-\frac{t}{\tau}} \sin \omega t \tag{5}$$

where τ=2L/R, ω is the zero phase angle frequency. $v_C(0)$ is the initial voltage at the switching transient. It can be seen that the solution to the track current for a direct AC-AC converter is time dependent during different energy injection periods.

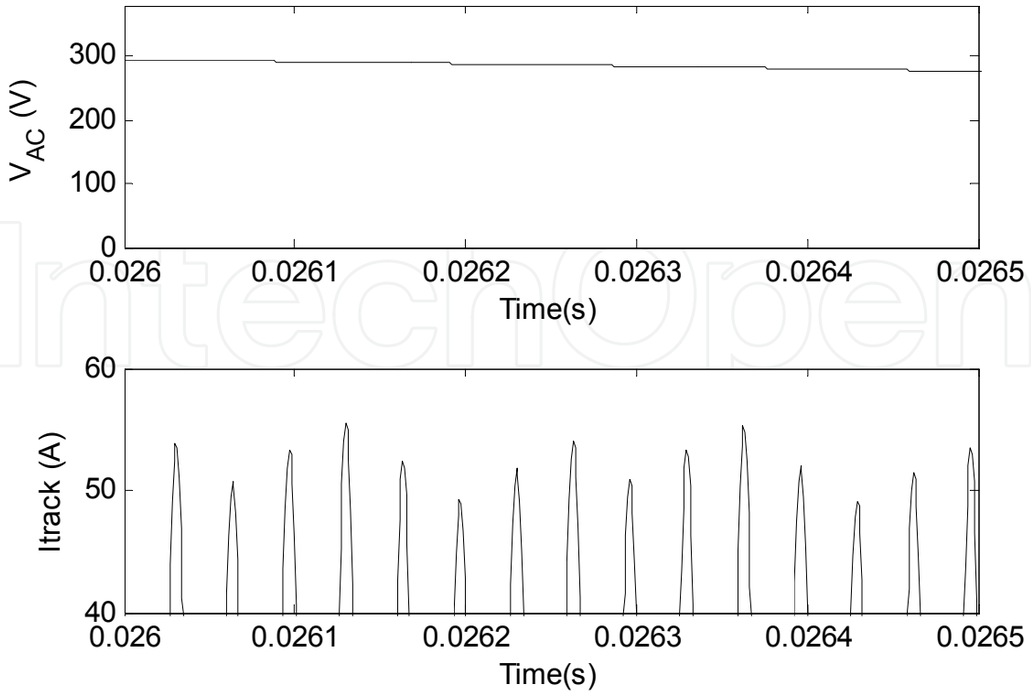

Fig. 11. Current ripples during controlled period.

Under the discrete energy injection control strategy with variable frequency switching, the current resonance can be well maintained, but over energy injection will also occur especially when the AC input voltage reaches its peak. F shows the typical waveform of the track current with a reference of the input voltage.
It can be seen that the current presents a small ripple around the reference current during the controlled period under steady state. The amount of energy injected into the circuit at different phase angle of the mains voltage varies and can be more than what is required to maintain a constant track current. Any over injection of energy during each injection period results in a current overshoot. Similarly, any over consumption during the oscillation period contributes to the current ripple.
An approximated worst case method can be used to find the maximum and minimum peak current of the AC-AC converter caused by the magnitude variation of the AC input. In order to clearly understand the current ripple under the controlled period, a detailed waveform showing the track current under the worst case conditions is given in Fig.12.

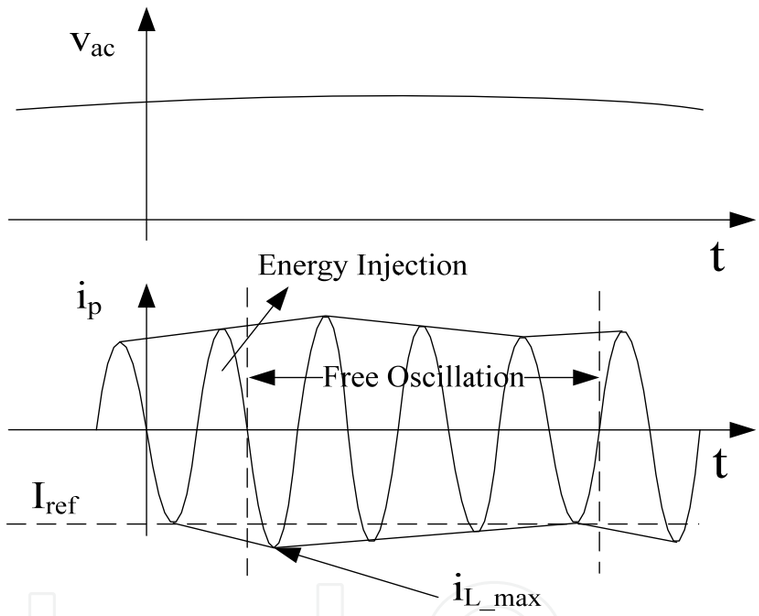

Fig. 12. A detail current ripple waveform.

It can be seen that during the control period, if the input voltage is at the positive cycle, the track current always enters the free oscillation state during its negative cycle. When the converter operates under free oscillation period, there is no energy injected. As a result, the track current is naturally damped by the load and ESR. If the peak current in the negative half cycle is slightly smaller than or equal to the reference value I_{ref}, energy will be injected by the controller into the resonant network in the next positive half cycle. With this energy injection, the current increase from zero to its peak during the positive cycle. Such a peak value will be larger than the previous negative peak value, but it is not the maximum value. This is because the energy will be continually injected during the remaining time of the entire positive cycle and after this positive peak value. In fact, the real maximum peak current i_{L_max} appears in the following negative half cycle as shown in the figure after the half energy injection period is complete.

As stated, in the worst case scenario under no load condition, the capacitor voltage will approximate to zero when the track current is at its peak. After the energy injection over half a period, the total energy storage in the circuit equals the stored energy, and the newly injected energy can be expressed as:

$$\frac{1}{2}L\hat{i}_{L\_\max}^{\ 2} = \frac{1}{2}LI_{ref}^{\ 2} + \int_0^{\frac{T}{2}} v_{in}(t)\cdot i_L(t)dt \tag{6}$$

An energy balance principle can be applied to any energy injection period. But the worst case occurs when the current is just smaller than Iref and energy is still being injected when the mains voltage is at its peak value as stated earlier.
As the frequency of the resonant current is much higher than the 50Hz input voltage, the voltage added to the resonant tank at the peak of 50 Hz can be approximately expressed as:

$$v_{in}(t) \approx \hat{V}_{AC} \tag{7}$$

Therefore the injected energy during the entire half period over the peak of the mains can be expressed by:

$$E_{in} = \int_0^{\frac{T}{2}} v_{in}(t)\cdot i_L(t)dt = \frac{\hat{V}_{AC}^{\ 2} + 2\pi f \hat{V}_{AC} I_{ref} L}{2\pi^2 f^2 C} \tag{8}$$

From (6) and (8), the maximum track current can be obtained as:

$$\hat{i}_{L\_\max} = \sqrt{I_{ref}^{\ 2} + \frac{2T\hat{V}_{AC}\sqrt{LC}\left(I_{ref}\sqrt{\frac{L}{C}} + \hat{V}_{AC}\right)}{\pi}} \tag{9}$$

It can be seen from equation (9) that the overshoot of the maximum track current is determined by the peak AC input voltage, the controlled reference current, the track current resonant frequency, and the circuit parameters.
Although the maximum peak current is caused by the energy injection, the minimum peak current i_{L_min} is caused by circuit damping. The worst case scenario arises when the load is at its maximum and the peak current is slightly larger than the reference value. Under such a condition there is no injection in the next half cycle. Strictly speaking when the current is at its peak, the capacitor voltage is not exactly zero due to the existence of the load resistance. But for inductive power transfer applications, the Q of the primary circuit is normally high so that the assumption of the initial conditions $i_L(0) = -I_{ref}$ and $v_C(0)=0$ does not cause any significant error. For the proposed AC-AC converter, if it is operated when the input voltage is in its positive cycle, the energy can only be injected in the following positive half cycle. The initial peak value under such a condition is equal to the reference value during negative cycles of the resonant current, and there is no energy injection in the following positive cycle of the current while the damping remains. Instead of damping in the positive half cycle, the damping of current would last for another negative half cycle. With such given initial conditions, the minimum peak current i_{L_min} can therefore be obtained as:

$$\hat{i}_{L\_\min} = I_{ref}\frac{\omega_0}{\omega}e^{-\pi R\sqrt{\frac{C}{L}}} \tag{10}$$

According to the structure and control strategy of the AC-AC converter, the minimum current can only happen in the negative cycles. It can be seen from equation (10) that the worst minimum peak current is determined by the reference current and the circuit parameters.

In addition to the current ripples caused by energy injection and energy consumption during the current controlled period, current sag occurs when the input voltage changes its polarity. Fig.13 shows the envelope of the typical current waveform when the input voltage changes from the positive half cycle to the negative half cycle. It can be seen that around the zero crossing point, the input voltage falls back to zero and the magnitude of voltage is very low. Consequently, there is not enough energy that can be injected to sustain the track current to be constant, even if the maximum possible energy is injected in every half cycle.

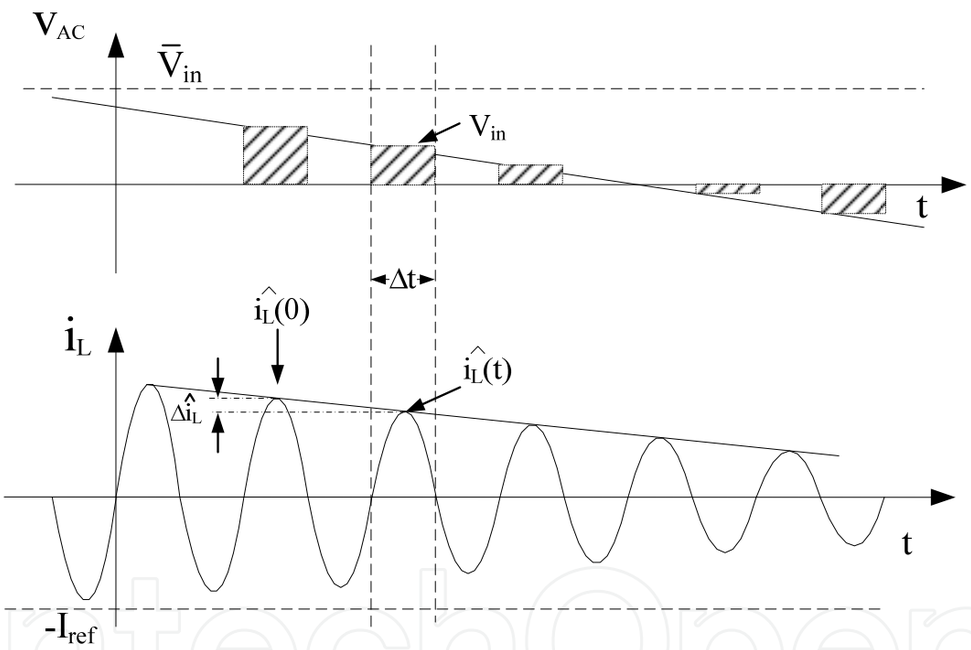

Fig. 13. Current sags around zero crossing point of the input voltage.

It can be seen that before the current sag occurs, the controlled current is around the reference value I_{ref} although small fluctuations exist due to the control. This means the input voltage is large enough to supply the energy to maintain a constant current around I_{ref}. However, over time, the input voltage drops to the boundary value, which is the minimum value to ensure the desired current without any control. This value can be obtained by:

$$\overline{V_{in}} = \frac{RI_{ref}\pi}{2} \tag{11}$$

Theoretically, if the input voltage is smaller than the boundary value, the newly injected energy will be too small to achieve the desired outcome and reaches zero when the input

voltage is at the zero crossing point. During this period, the injected energy in each positive half cycle can be calculated by:

$$E_{in} = \int_0^{\Delta t} v_{in}(t) i_L(t) dt = \frac{V_{in} \cdot \hat{i}_L \cdot \Delta t}{\pi} \tag{12}$$

Apart from this newly injected energy in each half cycle, there will be some stored energy in the resonant network because of the energy storage components. As discussed before, because of the high Q characteristic on the primary track, the phase angle of the resonant current and the capacitor voltage is very small and can be ignored. Therefore, the stored energy on the capacitor can be treated as zero when the resonant current is at its peak value. This stored energy in the tank can be expressed in terms of the inductance. At each positive half cycle, the instantaneous stored energy in the resonant tank can be calculated and expressed as:

$$E_{store} = \frac{1}{2} L \hat{i}_L(t)^2 \tag{13}$$

In order to identify the stored energy in different cycles, as shown in Fig. 13, the stored energy during the previous energy injection cycle is equal to:

$$E_{store} = \frac{1}{2} L \hat{i}_L(0)^2 \tag{14}$$

Since the difference in the peak current in two continuous positive half cycle is very small, the variation of the stored energy in one resonant period can be approximately expressed as:

$$\Delta E_{stored} = \frac{1}{2} L (\hat{i}_L(t)^2 - \hat{i}_L(0)^2) \approx L \cdot \Delta \hat{i}_L \cdot \hat{i}_L(t) \tag{15}$$

In addition to the variation in stored energy variation and the injected energy during the zero crossing periods, the energy is consumed by the load during on each half cycle. The consumed energy by the load during each resonant period can be expressed as:

$$E_{consumption} = \frac{\Delta t \cdot \hat{i}_L(t)^2 \cdot R}{2} \tag{16}$$

According to the energy balance principle, the injected energy during each cycle should be equal to the stored and consumed energy when the input voltage is around its zero crossing point. Thus, the equation for expressing the total energy balance in the resonant tank can be obtained as:

$$E_{in} = \Delta E_{store} + E_{consumption} \tag{17}$$

Substituting equation (12) to equation (17), the relationship between the minimum peak current and input voltage can be determined by:

$$\pi L \frac{\Delta \hat{i}_L}{\Delta t} + \frac{\pi}{2} R \hat{i}_L - V_{in} = 0 \tag{18}$$

Because $\Delta\hat{i}_L$ and Δt are very small, equation (18) can be expressed in the format of a differential equation as:

$$L\frac{d\hat{i}_L}{dt}+\frac{R}{2}\hat{i}_L-\frac{1}{\pi}V_{in}=0 \tag{19}$$

It can be seen from this equation that the analysis of the peak current of the track is simplified to a first order differential equation with initial values. The envelope can be presented according to the calculated solutions in the time domain.

The input voltage during the current controlled operation period can be modelled as a constant voltage $\overline{V_{in}}$ which is used to maintain the reference current I_{ref}. Therefore, the initial value of the envelope peak current is the reference current, before the voltage drops to zero from the boundary value $\overline{V_{in}}$. Around the zero crossing point of the mains voltage, the input voltage shows a good agreement with a ramp signal shown in Fig.14. It can be seen that the first trace is the approximated ramp input. In comparison, this ramp signal is compared to a 50 Hz input in the second figure. The error between each other is almost imperceptible during the zero crossing point of the input voltage.

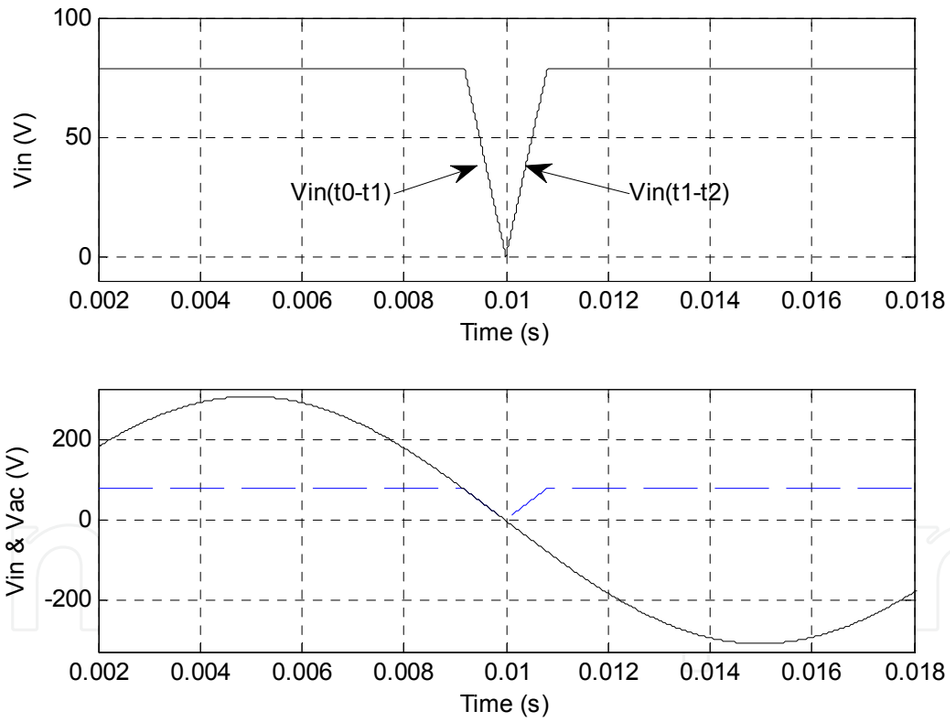

Fig. 14. Piecewise ramp input voltage.

As such, the input voltage of V_{in} around the zero crossing period can be approximated as a piecewise ramp input described by:

$$V_{in}(t_0-t_1)=\frac{RI_{ref}\pi}{2}\left[1-\frac{100\pi}{\arcsin(RI_{ref}\pi/2\hat{V}_{AC})}t\right] \tag{20}$$

and

$$V_{in}(t_1 - t_2) = \frac{50RI_{ref}\pi^2}{\arcsin(RI_{ref}\pi / 2\hat{V}_{AC})}t \tag{21}$$

A figure of the response envelope current with the piecewise input voltage is shown in Fig.15. In order to clearly see the envelope current obtained by equation (19) under the defined voltage of equation (20) and (21), the simulation results of track current by PLECS during the zero crossing point of the mains voltage is shown in the figure also.

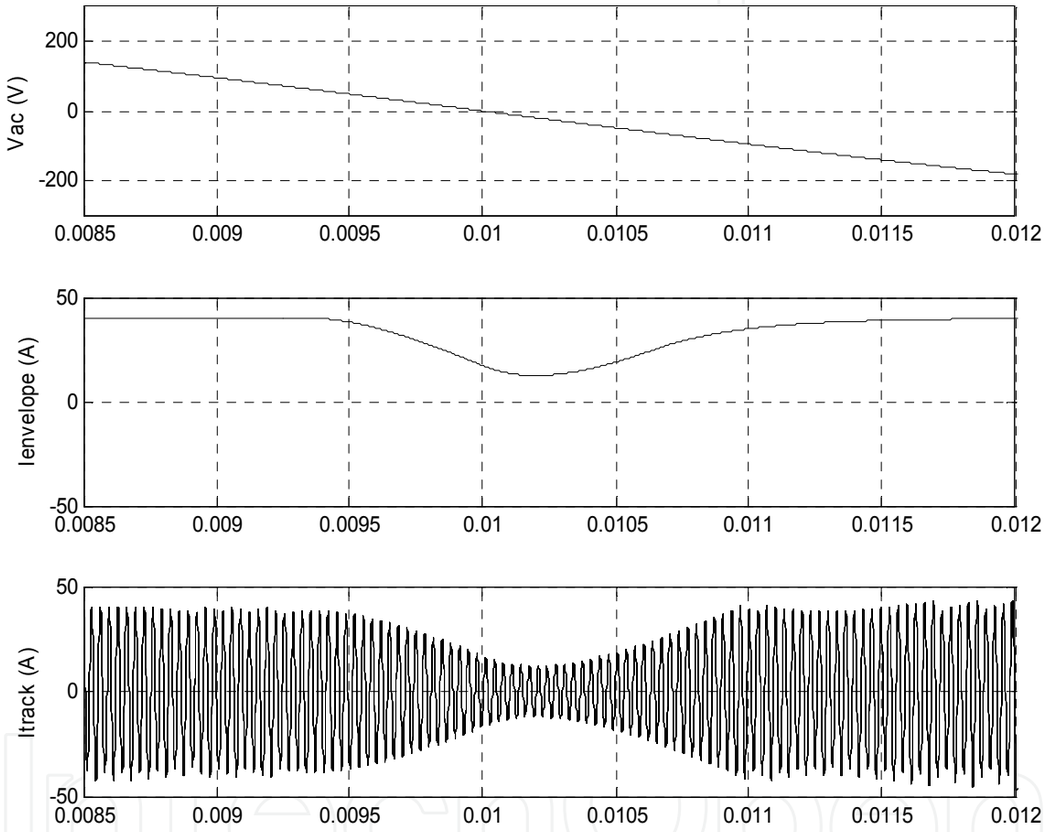

Fig. 15. Current sag during zero voltage crossing of mains: a) Calculated track current envelope, b) Simulated track current.

It can be seen that the envelope of the peak current described by equation (19) under the piecewise input voltage presents a good agreement with the envelope of the simulation track current. If the initial value of the peak current Iref is known, the analytical solution of the minimum value of the current can be obtained by solving equation (19), with the two given piecewise input functions (V_{in}(t0-t1),V_{in}(t1-t2)).
By solving equation (19) for the function of the first piecewise input yields:

$$I(t_1) = I_{ref}e^{-\frac{R}{2L}t_1} + K(t_1 - \frac{2L}{R} + \frac{2L}{R}e^{-\frac{R}{2L}t_1}) \tag{22}$$

Here, time $t_1 = \arcsin(RI_{ref}\pi / \hat{V}_{ac}) / 100\pi$. K is a constant which can be expressed by $K = -100\pi I_{ref} / \arcsin(RI_{ref}\pi / 2\hat{V}_{ac})$.

After obtaining the final value of the first damping ramp input, the final value of the first piecewise input will be the initial value for the next increasing ramp piecewise input voltage Vin(t1-t2). The solution of the current envelope during this time period of t1-t2 can be expressed by:

$$I(t) = K(t + t_1 e^{-\frac{R}{2L}t}) + \frac{2L}{R}(1 - e^{-\frac{R}{2L}t}) - \frac{2L}{R}e^{-\frac{R}{2L}t}(1 - e^{-\frac{R}{2L}t_1}) + I_{ref}e^{-\frac{R}{2L}(t_1+t)} \quad (t_1 < t < t_2) \tag{23}$$

It can be seen from Fig.14 that the second piecewise input voltage increases from zero to the reference value $\bar{V}_{in}$ during the time interval t1-t2, the current however reaches a minimum a short period after this. This is because initially the injected energy is very low and the consumed energy is larger than the injected energy. This means that the stored energy is needed to compensate for the over energy consumption. The total energy in the resonant tank would therefore decrease. With the voltage increasing, correspondingly the injected energy would increase. When the injected energy is larger than the energy consumption, the energy starts to increase. As a result the current envelope increases after reaching its minimum value. The exact time can be obtained during t1-t2 by taking:

$$I'(t) = 0 \tag{24}$$

Therefore the time of the minimum of the current envelope can be obtained as:

$$t_{\min} = -\frac{\ln\frac{K_1}{\tau K_2}}{\tau} \tag{25}$$

where τ=2L/R, $K_1 = K / L$ and $K_2 = 2K / R + I(t_1)$. After knowing the exact time at which the minimum peak current occurs, the minimum value can be obtained by substituting equation (25) into equation (23). The minimum sag current can then be expressed by:

$$\mathrm{I}_{\min} = \frac{2LK}{R} + \left[I_{ref}e^{-\frac{R}{2L}t_1} + K(t_1 - \frac{2L}{R} + \frac{2L}{R}e^{-\frac{R}{2L}t_1}) \right] \frac{2LK_1}{RK_2} \tag{26}$$

The minimum value of the current sag of the converter is related to the circuit parameters. Ideally, if the consumption is very low and the stored energy is very large, the exponential component has less effect. It requires a large primary Q to act as a filter for filtering off the low frequency components.

5. Simulation study

The simulation study of the AC-AC converter was undertaken using Simulink/PLECS to investigate the operation and analysis of the converter. The PLECS model of the AC-AC converter is shown in Fig.16.

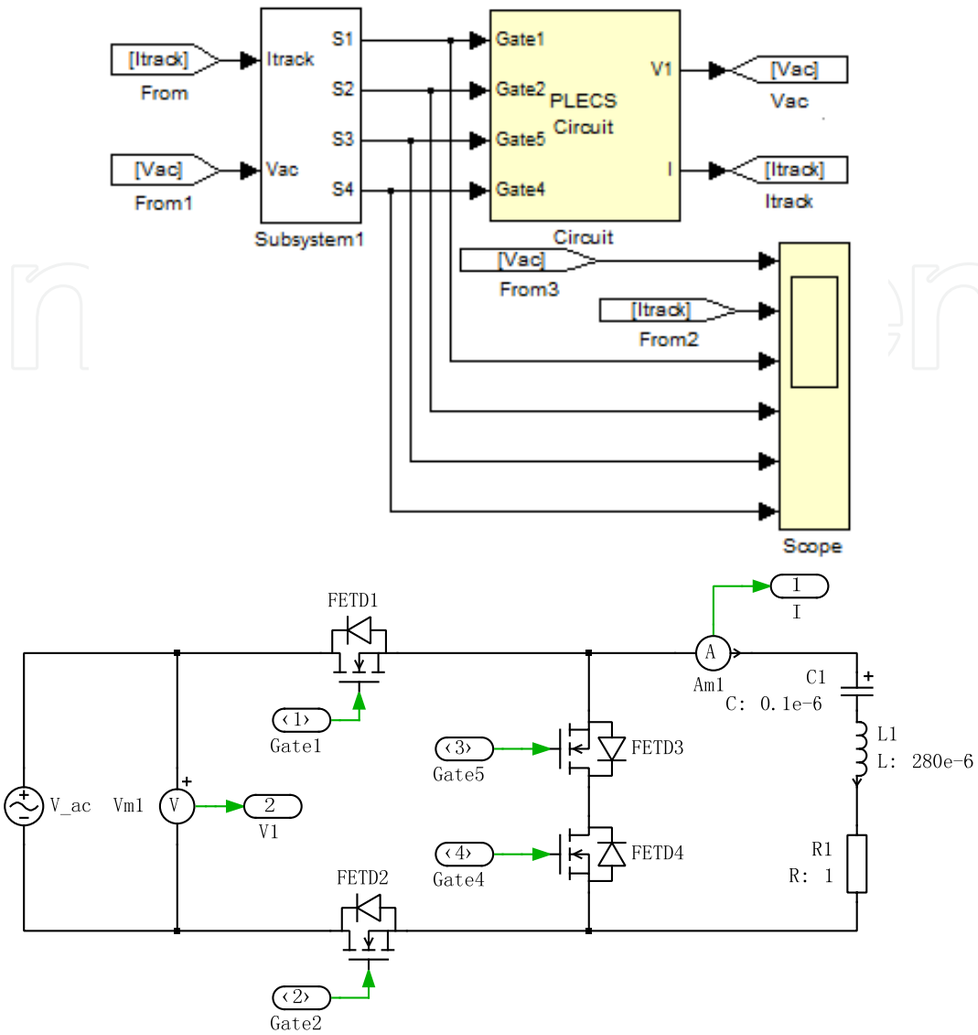

Fig. 16. PLECS circuit model of direct AC-AC converter.

It consists of four switches, an AC input source, and a tuning track. Gate control signals (gate1 to gate4) are fed in from the controller block. The input voltage and track current are measured and feed back to the controller. The converter is designed according to the parameters listed in Table 2.

Symbol	Notes	Value
f_0	Operating frequency of the converter	30 kHz
V_{AC}	Input voltage in RMS	220 V
f_{AC}	Frequency of AC input	50 Hz
L	Track Inductance	280 µH
C	Tuning capacitors	0.1 µF
R	Equivalent total Load	1 Ω
Iref	Track Current reference	40 A

Table 2. Converter circuit parameters of a direct AC-AC resonant converter.

Fig.17. shows the simulation results under variable frequency switching control, which include the waveforms of the input voltage V_{AC}, the track current (I_{track}), and the control signals of S1-S4.

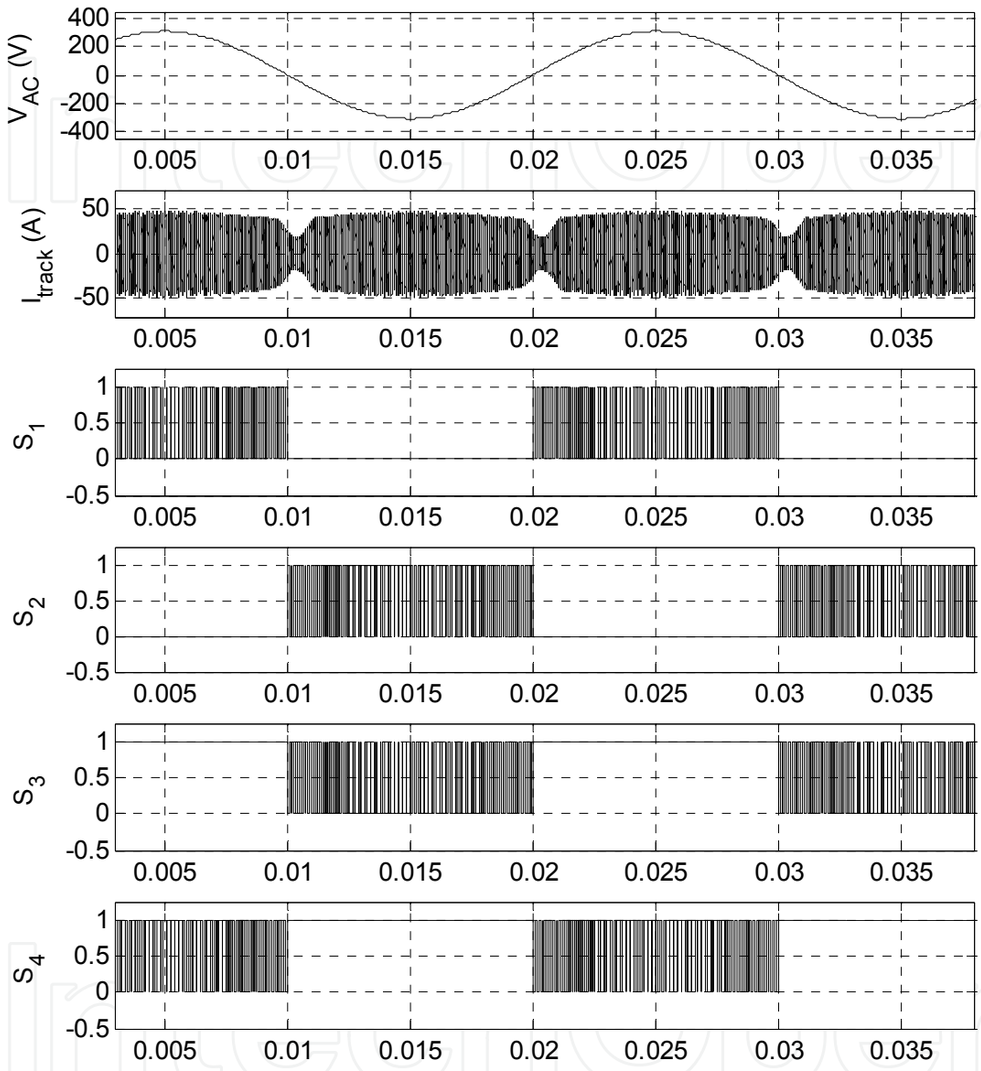

Fig. 17. Simulation waveform of a typical energy injection AC-AC converter.

It can be seen that a low frequency mains voltage can be used to generate a high frequency current for IPT applications under the proposed topology and operation of the AC-AC converter. From Fig. 17 S1 and S4 control the energy injection and the current oscillation when the input is in the positive direction. S2 and S3 control the energy injection and free oscillation during the negative direction of the input voltage. In addition, the switching commutation is achieved smoothly by the proposed switching control technique. The current waveform is controlled around the predefined reference some fluctuations including both the ripples during controlled period and the sages during zero crossing of the input voltage, which have been discussed and compared in the earlier analysis.

6. Conclusions

In this chapter, a direct AC-AC IPT converter has been proposed. The converter has been shown to have a simpler structure compared to a traditional AC-DC-AC converter. This chapter focused on the analysis of the AC-AC converter in relation to the control strategy.
While there are a number of possible topologies for the direct AC-AC converters based on energy injection and free oscillation technique as discussed, only one selected example converter topology is described here. The operation principle and a detailed switching control sequence with reference to the current waveforms were analyzed. System modeling and theoretical analysis on the performance of the direct AC-AC converter were also conducted; in particular, the current ripple analysis including the current fluctuation during normal operation was undertaken. In addition, the current sag around zero crossing points of the input voltage was analysed using energy balance principles. In the analysis, the approximate current envelope has also been derived to show the current sag. The validity of both the theoretical analysis and the control method has been verified by simulation studies.

7. References

Dawson, B. V., I. G. C. Robertson, et al. (1998). "Evaluation of Potential Health Effects of 10 kHz Magnetic Fields: A Rodent Reproductive Study."

Dissanayake, T. D., D. Budgett, et al. (2008). Experimental thermal study of a TET system for implantable biomedical devices. IEEE Biomedical Circuits and Systems Conference (BioCAS 2008).

Hisayuki, S., E. Ahmad Mohamad, et al. (2005). High frequency cyclo-converter using one-chip reverse blocking IGBT based bidirectional power switches. Proceedings of the Eighth International Conference on Electrical Machines and Systems.

Hu, A. P., J. T. Boys, et al. (2000). ZVS frequency analysis of a current-fed resonant converter. 7th IEEE International Power Electronics Congress, Acapulco, Mexico.

Kaiming, Y.&L. Lei (2009). Full Bridge-full Wave Mode Three-level AC/AC Converter with High Frequency Link. IEEE Applied Power Electronics Conference and Exposition (APEC 2009).

Kissin, M. L. G., J. T. Boys, et al. (2009). "Interphase Mutual Inductance in Poly-Phase Inductive Power Transfer Systems." IEEE Transactions on Industrial Electronics.

Li, H. L., A. P. Hu, et al. (2009). "Optimal coupling condition of IPT system for achieving maximum power transfer." Electronics Letters 45(1): 76-77.

Sugimura, H., M. Sang-Pil, et al. (2008). Direct AC-AC resonant converter using one-chip reverse blocking IGBT-based bidirectional switches for HF induction heaters. IEEE International Symposium on Industrial Electronics.

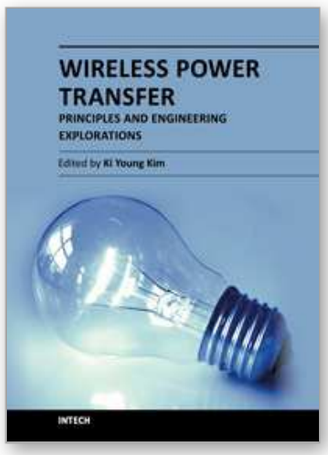

Wireless Power Transfer - Principles and Engineering Explorations
Edited by Dr. Ki Young Kim

ISBN 978-953-307-874-8
Hard cover, 272 pages
Publisher InTech
Published online 25, January, 2012
Published in print edition January, 2012

The title of this book, Wireless Power Transfer: Principles and Engineering Explorations, encompasses theory and engineering technology, which are of interest for diverse classes of wireless power transfer. This book is a collection of contemporary research and developments in the area of wireless power transfer technology. It consists of 13 chapters that focus on interesting topics of wireless power links, and several system issues in which analytical methodologies, numerical simulation techniques, measurement techniques and methods, and applicable examples are investigated.

How to reference
In order to correctly reference this scholarly work, feel free to copy and paste the following:

Hao Leo Li, Patrick Aiguo Hu and Grant Covic (2012). A High Frequency AC-AC Converter for Inductive Power Transfer (IPT) Applications, Wireless Power Transfer - Principles and Engineering Explorations, Dr. Ki Young Kim (Ed.), ISBN: 978-953-307-874-8, InTech, Available from: http://www.intechopen.com/books/wireless-power-transfer-principles-and-engineering-explorations/a-high-frequency-ac-ac-converter-for-inductive-power-transfer-ipt-applications

INTECH
open science | open minds

InTech Europe
University Campus STeP Ri
Slavka Krautzeka 83/A
51000 Rijeka, Croatia
Phone: +385 (51) 770 447
Fax: +385 (51) 686 166
www.intechopen.com

InTech China
Unit 405, Office Block, Hotel Equatorial Shanghai
No.65, Yan An Road (West), Shanghai, 200040, China
中国上海市延安西路65号上海国际贵都大饭店办公楼405单元
Phone: +86-21-62489820
Fax: +86-21-62489821

IntechOpen